

Intrinsic Capacity of the MIMO Wireless Channel

Jon W. Wallace and Michael A. Jensen*
 Department of Electrical and Computer Engineering
 Brigham Young University, 459 CB, Provo, UT 84602
 wallacej@ee.byu.edu, jensen@ee.byu.edu

I. Introduction

Information theoretic analyses and real propagation measurements [1]-[3] have demonstrated the capacity advantage of multiple-input multiple-output (MIMO) systems over single-antenna networks for wireless communications over multipath channels. In these studies, the “channel” consists of a fixed physical propagation environment and antenna array configuration. Because the capacity computed for these channels depends on the antenna physical characteristics, it does not represent a true upper bound on achievable performance for a specific channel. This bound is important as, without it, no true definition of optimality for MIMO communications is possible.

In this work, we propose a new framework for computing the capacity of electromagnetic channels that is independent of the transmit and receive antenna characteristics. Given a realistic channel model and very general operational principles of the antenna elements, this framework yields the *intrinsic capacity* representing the maximum mutual information over *all* possible transmission system parameters (including antenna configurations). This metric therefore provides an ultimate upper bound on antenna array performance for MIMO systems and defines a point of diminishing returns for effort in physical antenna design.

II. Channel Model

Consider a single-user continuous-space electromagnetic channel characterized by transmit (*source*) and receive (*sensor*) volumes $\Delta V'$ and ΔV respectively. It is assumed that we know the generalized dyadic Green's function $\bar{\bar{h}}_{rt}(\bar{r}, \bar{r}')$ describing the fields generated in ΔV due to the sources in $\Delta V'$. Given that a practical system has a finite number of data streams at the transmitter and field measurements at the receiver, it is logical to pursue the development using properly normalized source and sensor basis functions $T_i(\bar{r}')$ and $R_k(\bar{r})$ respectively. Using this notation, the k th sensor records the generalized voltage measurement

$$Y_k = \int_{\Delta V} d\bar{r} \int_{\Delta V'} d\bar{r}' \left[\bar{R}_k^H(\bar{r}) \bar{\bar{h}}_{rt}(\bar{r}, \bar{r}') \sum_i X_i \bar{T}_i(\bar{r}') \right] + N_k = \sum_i H_{ki} X_i + N_k \quad (1)$$

where X_i is the complex weight applied to the basis function T_i and N_k is measurement noise or error. Therefore, for fixed basis functions, the capacity for the channel represented by $\bar{\bar{H}}$ can be computed using standard techniques [2], [4]. However, this analysis only produces the intrinsic capacity if the optimal set of basis functions is used.

Unfortunately, for general channels with the sources and sensors confined to finite apertures, there does not appear to be a mechanism for constructing the optimal basis functions to use in capacity computations. Therefore, we propose a simple numerical method that produces close approximations to these functions. To this end, consider defining sub-basis functions that span the transmit and receive spaces in a limiting sense as the number of sub-basis functions becomes infinite, or

$$\bar{T}_i(\bar{r}') = \sum_n c_{ni} \bar{T}_n(\bar{r}') \quad \bar{R}_k(\bar{r}) = \sum_n b_{nk} \bar{R}_n(\bar{r}). \quad (2)$$

If these sub-basis functions are orthonormal, then substitution of these expressions into (1)

results in

$$\begin{aligned} H_{ki} &= \int_{\Delta V} d\vec{r} \int_{\Delta V'} d\vec{r}' \left[\sum_m b_{mk} \overline{\mathcal{R}}_m(\vec{r}_r) \right]^H \overline{h}_{\pi}(\vec{r}_r, \vec{r}_i') \sum_n c_{ni} \overline{\mathcal{T}}_n(\vec{r}_i') \\ &= \sum_m \sum_n b_{mk}^* \mathcal{H}_{mn} c_{ni}. \end{aligned} \quad (3)$$

Representing the matrix $\overline{\mathcal{H}}$ in terms of its singular value decomposition (SVD) $\overline{\mathcal{H}} = \overline{U} \overline{S} \overline{V}^H$ and performing the substitutions $c_{ni} = v_{ni}$ and $b_{km} = u_{km}$ yield $H_{ki} = \delta_{ki} S_{kk}$. Also, since the sub-basis functions were constrained to be orthonormal, this assignment ensures that the transmit and receive basis functions are also orthonormal. In this case, the expression for mutual-information of the vectors \vec{Y} and \vec{X} becomes

$$I(\vec{Y}; \vec{X}) \leq \log_2 \left| \frac{\overline{S} \overline{k}_x \overline{S}}{\sigma_N^2} + \overline{I} \right| \quad (4)$$

where \overline{k}_x is the transmit covariance matrix and σ_N^2 is the single receiver noise variance. Equality in (4) is attained for complex Gaussian signaling, and the intrinsic capacity results if \overline{k}_x is chosen to maximize the expression [4].

III. Radiated Power Constraint

Maximization of (4) must be performed in conjunction with a constraint on the total power radiated by the sources. From a practical standpoint, this transmit power constraint should have a true physical interpretation. In many physical problems, instantaneous radiated power is related to the complex transmit element voltages or currents according to the relation $P_{\text{rad}} = \vec{X}^H \overline{A} \vec{X}$, where \overline{A} is a Hermitian *coherence matrix* and \vec{X} is the vector of transmit element voltages or currents. For example, if the sources consist of Hertzian dipoles such that the coefficient X_i represents the excitation on the i th antenna, then such a relation results from coherently summing the radiation from each dipole (array factor) and integrating the resulting far-field power density. A similar derivation can be performed for the sub-basis sources in (2). When this relation holds, the average radiated power is given as

$$E\{P_{\text{rad}}\} = E\{\vec{X}^H \overline{A} \vec{X}\} = \text{Tr}(\overline{k}_x \overline{A}) = P_T. \quad (5)$$

The maximization of (4) subject to (5) must be carefully performed due to the possible poor conditioning of \overline{A} . However, since “directions” of zero power radiated in \overline{A} must correspond to “directions” of zero signal transfer through \overline{H} , this difficulty can be overcome as follows. If $\overline{S} = \text{diag}(\overline{S})$ and the singular values are ordered from largest to smallest, we now consider only the N_S largest singular values that satisfy $S_1/S_i < \rho$, where ρ is some maximum allowed conditioning number. The matrices \overline{k}_x , \overline{S} , and \overline{A} are then truncated to contain only the leading N_S rows and columns, ensuring that \overline{A} has suitable conditioning. Next, we apply the substitution

$$\overline{k}_x = \overline{S}^{-1} \overline{\xi}_Z \overline{\Lambda}_Z^{-1/2} \overline{k}_x \overline{\Lambda}_Z^{1/2} \overline{\xi}_Z^H \overline{S}^{-1}, \quad (6)$$

where we have performed the eigenvalue decomposition (EVD) of $\overline{S} \overline{A}^{-1} \overline{S} = \overline{\xi}_Z \overline{\Lambda}_Z \overline{\xi}_Z^H$, which transforms the mutual information expression to

$$I(\vec{Y}; \vec{X}) = \log_2 \left| \frac{\overline{\Lambda}_Z^{1/2} \overline{k}_x \overline{\Lambda}_Z^{1/2}}{\sigma_N^2} + \overline{I} \right| \quad (7)$$

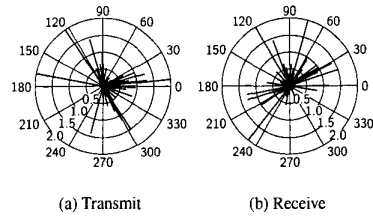


Figure 1: Transmit and receive ray structure in the horizontal plane generated with a single realization of the channel model. Each impulse corresponds to a ray in the specified direction with an amplitude equal to the impulse length.

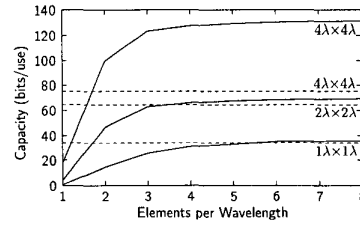


Figure 2: Intrinsic capacity versus the sampling resolution for box-shaped sub-basis elements. Capacity of the fixed 16-element square dipole array (dashed lines) is shown for comparison.

and the power constraint to simply $\text{Tr}(\bar{\mathbf{k}}_x^Z) = P_T$. This problem is now in a form to which the water-filling solution approach is applicable.

IV. Intrinsic Capacity Computations

The analysis of a full vectorial three-dimensional scenario is very complicated and tends to obscure the basic technique. Therefore, we assume a very simple single-polarization two-dimensional path-based ray model for the following computations [3], [5]. The intrinsic capacity framework has been applied to sub-basis functions that divide the allowed antenna volumes into non-overlapping boxes. The capacity of a square array of 16 Hertzian dipoles placed around the perimeter of the transmit and receive (square) apertures has also been formulated for comparison. In this latter example, however, the effective area of the receive dipoles is limited so that the antenna cannot collect more power than a box-shaped sub-basis element occupying the same volume. The choice of 16 dipole antennas is somewhat arbitrary, but provides a baseline for comparison between fixed array and intrinsic capacity computations. The single-element receiver noise power is fixed assuming a single-input single-output signal-to-noise ratio of 20 dB. Fig. 1 shows the angle of departure/arrival as well as the relative magnitudes of the multipath components used.

Figure 2 plots the intrinsic capacity estimates given by the box-shaped sub-basis as a function of the number of sub-basis sources/sensors per wavelength. Three different allowed antenna areas ($\Delta x \times \Delta y$) were simulated: $1\lambda \times 1\lambda$, $2\lambda \times 2\lambda$, and $4\lambda \times 4\lambda$. The capacity of the fixed 16-element square array for each area is also provided for comparison (the dashed horizontal lines). The results show that the capacity of the boxed-shaped sensors approaches a horizontal asymptote (the intrinsic capacity) as the sampling resolution increases. A good estimate of the intrinsic capacity is reached for about 6 elements per wavelength. Also, for small antenna area, the 16-element array nearly achieves the intrinsic capacity limit. However, for larger areas, the discrepancy widens. The difference is due to the fact that for the square array: (1) for large areas the fields are undersampled, and (2) the power collection capability for a fixed number of dipoles is inherently limited.

Combining many realizations of the channel model with the Monte Carlo technique provides insight into the statistical behavior of the intrinsic capacity. Here, box-shaped sensors with a sampling resolution of 8 sensors per wavelength were used to provide close estimates of the intrinsic capacity. 5000 channel realizations were generated to approximate each probability distribution.

Figure 3 depicts complimentary cumulative distribution functions (CCDFs) of intrinsic capac-

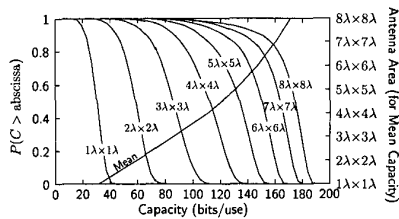


Figure 3: Estimates of the intrinsic capacity CCDFs and mean intrinsic capacity versus allowed antenna area

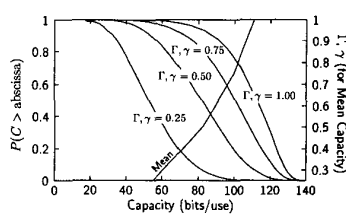


Figure 4: Estimates of the intrinsic capacity CCDFs and mean intrinsic capacity versus channel model multipath parameters Γ and γ

ity and mean intrinsic capacity versus the allowed antenna area ($\Delta x \Delta y$). The model parameters and therefore available multipath were fixed in these simulations. For a small antenna area, the capacity increases almost linearly with the allowed antenna dimensions. As the antenna dimensions increase, however, the intrinsic capacity approaches an upper bound.

Figure 4 plots CCDFs of intrinsic capacity and mean intrinsic capacity versus the multipath parameters Γ and γ , with larger values of Γ and γ corresponding to more available multipath. The antenna area is fixed at $4\lambda \times 4\lambda$ with 8 box-shaped elements per wavelength. As before, 5000 realizations were performed to estimate each probability distribution. This study demonstrates that antenna aperture strongly limits the intrinsic capacity, even when the available multipath grows large.

V. Conclusion

This paper has presented a new framework for analysis of the continuous-space electromagnetic channel, defining an ultimate upper bound on the available capacity for constrained antenna volumes, radiated power, and receiver noise. We have defined this capacity bound as “intrinsic capacity” since it represents a capacity limitation of the physical propagation environment that is independent of the system-specific antennas and array geometries. Representative simulations compared the intrinsic capacity bound with a physically realizable array and demonstrated the statistical behavior as a function of the allowed antenna volume and available multipath.

Acknowledgements: This work was supported by the National Science Foundation under Wireless Initiative Grant CCR 99-79452 and Information Technology Research Grant CCR-0081476.

References

- [1] G. J. Foschini and M. J. Gans, “On limits of wireless communications in a fading environment when using multiple antennas,” *Wireless Personal Communications*, **6**, pp. 311–335, 1998.
- [2] G. G. Rayleigh and J. M. Cioffi, “Spatio-temporal coding for wireless communication,” *IEEE Trans. Commun.*, **46**, pp. 357–366, 1998.
- [3] J. W. Wallace and M. A. Jensen, “Statistical characteristics of measured MIMO wireless channel data and comparison to conventional models,” in *IEEE VTC’2001 Fall Conf.*, **2**, pp. 1078–1082, Atlantic City, NJ, 2001.
- [4] T. M. Cover and J. A. Thomas, *Elements of Information Theory*, John Wiley & Sons, 1991.
- [5] Q. Spencer, B. Jeffs, M. Jensen, and A. Swindlehurst, “Modeling the statistical time and angle of arrival characteristics of an indoor multipath channel,” *IEEE J. Selected Areas Commun.*, **18**, pp. 347–360, 2000.